FACTA UNIVERSITATIS
Series:**Mechanical Engineering**
https://doi.org/10.22190/FUME211214016S

Original scientific paper

EXPERIMENTAL AND NUMERICAL STUDY OF THE IMPACT OF THE OIL TANK FILLING LEVEL ON THE AIRCRAFT SEPARATOR

Tomasz Szwarc[1,2], Włodzimierz Wróblewski[1], Tomasz Borzęcki[2]

[1]Silesian University of Technology, Poland
[2]Avio PolskaSp. z o.o., Poland

Abstract. *This paper presents a CFD analysis of an air-oil separator of an aircraft gas turbine engine with a focus on the impact of the oil tank filling level on the separator performance for a selected point of the flying mission. The separator efficiency and the oil quality affect the efficiency of the oil system. New design criteria and standards require a better understanding of the phenomena occurring in the separator. To optimize its structure, the flow of the air-oil mixture must be modeled in the design process. Although many papers are addressing the issue of gas-liquid separation, very little knowledge is available on the flow ratio typical of aircraft turbine engines. The separation phenomena were investigated using the volume-of-fluid method. Transient calculations were performed at a selected mission point of the separator and compared with experimental data. A mesh independence study using a structural mesh is included to understand the mesh impact on the analysis results. The current analysis results will support further studies focusing on an optimization analysis where a proper mesh, an adequate turbulence model and an appropriate oil level have to be selected.*

Key Words: *Multiphase Flow, Air-oil Separator, Cyclone, Volume of Fluid Method*

1. INTRODUCTION

Secondary air and lubrication systems have a decisive influence on the characteristics and operational capabilities of aircraft engines. The characteristics of these two systems define the mixture volume ratio, which depends on the flight mission conditions. During the engine operation, the oil tank level changes due to the gulping effect, engine oil hiding and attitude. These phenomena affect separation efficiency and change the flow field formation. The separator performance has a decisive impact on the oil quality, directly affecting the oil system elements and the engine thermal capability. The oil flow

*Received: December 14, 2021 / Accepted March 27, 2022
Corresponding author: Tomasz Szwarc
Silesian University of Technology, ul.Grażyńskiego 141, Bielsko Biała 43-300
E-mail: tomasz.szwarc@avioaero.it

loss can also cause overheating due to the reduced heat transfer in the oil cooler, caused by low thermal capacity of the air. Other issues are related to the oil tank. Due to foam formation, the oil level can be indicated wrongly. Increased foaming can lead to high internal pressures causing seepage from connections or even resulting in the tank rupture in the worst case.

The most affected component of the lube system is an oil pump unit. A 1-2% air volume fraction in the oil system can affect the functioning of the gear pump at a high altitude and high-power operation. Vapor locked in the lube element area can cause cavitation while the creation of air-oil-metal interfaces inside the engine can be the starting point for corrosion. The influence on volumetric efficiency is still part of contemporary research [1].

Oil aeration problems were studied in the past and are investigated nowadays [2]. The oil aeration problem can be resolved in several different ways. A patent solution was proposed in [3] by adding an oil injection passage downstream of the pump to avoid recirculation of air bubbles in the gear meshing area. Another way is to decrease the scavenge pump discharge pressure by decreasing inlet losses or by using an oil type with suitable anti-foaming additives [2]. It prevents the formation of fine bubbles, which are the hardest to separate. Other mechanical routines of removing the gas entry can be obtained by designing a scavenge line with a velocity below 5 ft/s. The last approach is to increase radial acceleration and centrifugal force in the cyclone separator. It is a lube system component installed inside the engine oil tank. The major advantage of this component is its reliable structure. The deaerator must be designed to keep a good balance between the increase in the oil mixture velocity and the pressure drop. Overcoming pressure losses can cause issues during the engine cold start or can affect the design of the scavenge pump.

In the cyclone separator, the air-oil mixture flows through a tangential inlet slot. As a result, a swirl is generated causing the air to separate due to the centrifugal force. Regarding the separation phenomena on the wall, the air bubbles leave the oil particles and form foam. Due to the changes in the oil density and viscosity, small bubbles need more time to reach the free surface. Experimental data show that the bubbles do not rise so rapidly in the oil containing appropriate additives. Continuing the flow, the oil moves towards the wall and downwards while the air flows to the centre line and exits through the vortex finder. Depending on operating conditions, some oil droplets flow with the air and move up towards the air core. This phenomenon is called the liquid carry-over. At the bottom exit, air bubbles can remain in the oil and exit the tank. This phenomenon is called the gas carry-under [4]. Compared to typical industrial cyclone separators, those used in an aircraft need to meet more requirements. Changing operating conditions during flight missions involve changes in many parameters like the air-oil ratio, the oil tank filling level, the tank pressure, and the aircraft position (attitude). A highly swirling flow inside the separator is frequent and unsteady. The unstable flow field determines the separation performance. Another problem of the aircraft separator is its small volume, which makes the device very sensitive to variations in the flow parameters, such as the inlet flow pattern, or tangential and axial velocities. This can degrade the separation performance, which can cause operational problems [5].

Considering the existing available publications on aircraft cyclone separators, it can be stated that not many of them focus on performance [6]. The works presenting the state of the art in industrial cyclone separators [7-9] focus on a closed conical shape

(Stairmand, Stern or Lapple), which is often impossible to implement due to the limited design space. Moreover, the mathematical models of cyclone separators based on such research are limited to the single-phase flow or the dispersed-oil phase.

The studies on the fluid dynamic phenomena related to the air-oil flow in a gas turbine system recognize that the gas-liquid cylindrical cyclones (GLCC) used in the oil and gas industry behave in a similar way [10, 11]. Through systematic experiments and research performed in the past [12-17], detailed mechanistic models have been developed to describe important separation phenomena. Following the above, an approach intended for the air-oil separator used in the aircraft oil system is under preparation.

Based on experimental data, a theoretical study and a mechanistic model were developed to predict the operational envelope for the liquid carry-over and bubble trajectories [5, 14] for the GLCC. As indicated by the literature results, the turbulent swirling flow in cyclone separators is anisotropic [16]. Therefore, an anisotropic turbulence model should be used to model such a flow accurately. In other studies [4,16] different turbulence models were used to investigate the sensitivity of the flow field predictions. Using a Reynolds stress model, which is an anisotropic turbulence model, the simulations presented in [7-9] showed only a slight improvement over the k-ε model prediction of the flow field in the GLCC. Erdal and Shirazi [16] compared experimental results with a 3D CFD simulation. In the simulation, k-ε and RSM turbulence models were used. The analysis shows a general trend of experimental data but both models fail to predict certain parameters. The k-ε model tends to predict a higher rotational flow, whereas the RSM model predicts a different wavelength of the vortex and local axial and tangential velocities.

The most often used numerical modeling method aiming to describe the two-phase flow in separators is presented in [18]. The application of an appropriate numerical model is conditioned by the existence of a specific two-phase flow pattern, which should be identified or assumed based on experimental knowledge and maps of the flow pattern. The volume of fluid (VoF) is a free-surface modeling technique, which makes it possible to track the air-oil interface [19]. The interface between the phases is tracked using the continuity equation for the volume fraction. The volume fraction equation is not solved for the primary phase. As the volume of a phase cannot be occupied by other phases, the balance calculations are carried out for a given phase considering the volume fractions. A single momentum equation is solved throughout the domain, and the resulting velocity field is shared among the phases. The momentum equation is dependent on the volume fractions of all phases through the mixture density and mixture viscosity.

The initial numerical analyses of the oil separator investigated are presented in [20]. The calculations were performed using the VOF model and RNG k-ε turbulence model. These analyses were conducted for other definitions and discretization of the calculation domain. A tetragonal numeric grid was applied. The results of the calculations were compared with the experimental data for the adopted boundary conditions; it was found out that the chosen numeric models predict oil quality and performance correctly but do not have a complex domain enabling stabilization of the oil level.

This paper presents an analysis based on a separator used in the aircraft gas turbine engine. The objective of this study is to investigate tank oil level impact on separator performance. The computed separator parameters – oil quality and efficiency were compared with available experimental data to validate the model. Additionally, the impact of the oil level in the tank on the flow field below the separator inlet was investigated. The observed flow field phenomenon was compared to other separator types available in the industry.

2. MODELS AND METHODS

2.1 Mathematical model

Turbulence was simulated using the RNG k-ε model. The model is derived from the instantaneous Navier-Stokes's equations using a mathematical technique known as the "renormalization group" (RNG) method. It is based on the standard k-ε model but includes refinement. An additional term in the ε equation improves the accuracy for rapidly strained flows. Due to that, the effect of swirl on the turbulence is included, enhancing the accuracy for swirling flows. The RNG theory provides an analytical formula for the turbulent Prandtl numbers, while the standard k-ε model uses user-specified, constant values [21]. The equations for turbulence kinetic energy k and the dissipation rate of turbulent kinetic energy ε are solved:

$$\frac{\partial}{\partial t}(\rho k) + \frac{\partial}{\partial x_i}(\rho k U_i) = \frac{\partial}{\partial x_j}\left(\alpha_k \mu_{eff} \frac{\partial k}{\partial x_j}\right) + G_k - \rho \tag{1}$$

$$\frac{\partial}{\partial t}(\rho \varepsilon) + \frac{\partial}{\partial x_i}(\rho \varepsilon U_i) = \frac{\partial}{\partial x_j}\left(\alpha_\varepsilon \mu_{eff} \frac{\partial \varepsilon}{\partial x_j}\right) + C_{1\varepsilon}\frac{\varepsilon}{k}G_k - C_{2\varepsilon}\rho\frac{\varepsilon^2}{k} - R_\varepsilon \tag{2}$$

In the above equations, α_k and α_ε are the inversed effective Prandtl numbers for k and ε, respectively. $C_{2\varepsilon}$ and $C_{2\varepsilon}$ are constant values of 1.42 and 1.68, respectively. The scale elimination procedure in the RNG theory results in a differential equation for turbulent viscosity. In the high range of the Reynolds number, effective viscosity μ_{eff} is expressed as:

$$\mu_{eff} = \rho C_\mu \frac{k^2}{\varepsilon} \tag{3}$$

with C_μ=0.0845 derived using the RNG theory. It is interesting to note that this value of C_μ is very close to the empirically determined value of 0.09 used in the standard k-ε model.

The two-phase flow was modeled using the volume-of-fluid method [19]. The model type was chosen due to the possibility of creating a free surface between air and oil. This is an important feature considering the oil reservoir included in the simulation. The free surface will make it possible to determine the oil level in the tank and its influence on the separator operation. The continuity equation is solved:

$$\frac{\partial}{\partial t}(\rho) + \nabla \cdot (\rho \vec{v}) = 0 \tag{4}$$

where ρ is the mixture density calculated from:

$$\rho = \alpha_a \rho_a + (1 - \alpha_a)\rho_o \tag{5}$$

where ρ_a, ρ_o are densities of air and oil, respectively, and α_a is the volume fraction of air which is, in this case, the second phase.

$$\frac{\partial}{\partial t}(\alpha_a \rho_a) + \nabla \cdot (\alpha_a \rho_a \vec{v}_a) = \dot{m}_{oa} - \dot{m}_{ao} \tag{6}$$

where $\dot{m}_{oa}$, $\dot{m}_{ao}$ are mass transfer from oil to air and air to oil, respectively.

The volume fraction equation is not solved for the oil phase (primary), and the oil-phase volume fraction is computed based on the following constraint:

$$\alpha_a + \alpha_o = 1 \tag{7}$$

For this case, the volume fraction equation is solved through an implicit formula. A single momentum equation is solved throughout the domain, and the resulting velocity field is shared among the phases. The momentum equation, shown below, is dependent on the volume fractions of all phases through quantities ρ and μ.

$$\frac{\partial}{\partial t}(\rho\vec{v}) + \nabla \cdot (\rho\vec{v}\vec{v}) = -\nabla p + \nabla \cdot \left[\mu_{eff}(\nabla\vec{v} + \nabla\vec{v}^T)\right] + \rho\vec{g} + \vec{F} \tag{8}$$

2.2 Numerical model

The geometry of the calculation domain was created based on the geometry of an existing test bench, where the separator was installed in a cylindrical tank shown in Fig. 1.The calculation domain was simplified to improve the mesh quality and to decrease the number of elements. Rig connections like bolts and fittings were removed or simplified, and the fillet radius of the edge of the components was eliminated.

The temperature of the mixture is constant; there is no heat exchange with the surroundings. Considering together the calculations performed with structure maps and the close distance from the scavenge pump, it was possible to assume a uniform phase distribution. At the inlet, the mass flow rates of both air and oil were applied as boundary conditions. These values were set on the rig. The boundary condition at the separator outlet is defined by the scavenge pump characteristic. It is also essential that the outlet boundary conditions are determined correctly. The selected conditions must allow the occurrence of phenomena such as the liquid carry-over and the gas carry-under, where the outflow of air and oil can occur with different ratios. The problem was resolved by defining static pressures at the outlet boundaries since these values were monitored. The oil properties in the simulation were selected for a specific temperature. The test bench parametrized dimensions are listed in Table 1.

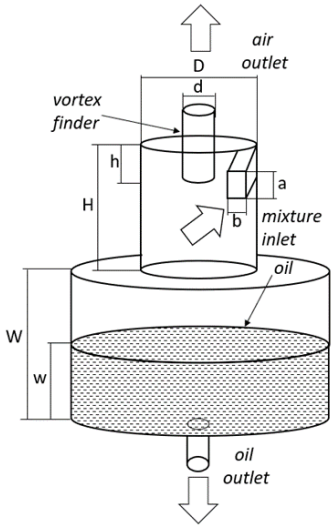

Fig. 1 Separator with tested oil tank

Table 1 Cyclone dimensions in reference to inlet tube height (a)

Cyclone height (H)	Vortex finder height (h)	Cyclone diameter (D)	Vortex finder diameter (d)	Inlet tube height (a)	Inlet tube width (b)	Tank height (W)
3.2	1.4	3.6	1.3	1	1.6	12

The numerical schemes for the current analysis were selected based on the analysis performed in [20, 22], but this analysis was conducted using a transient approach. A coupled scheme was selected as the algorithms for the pressure-velocity coupling. A "no-slip" wall boundary condition is assumed. The time step used in the simulations was related to the global Courant number. At the beginning of the simulation when the tank was being filled with oil, it was important to keep the Courant number low at ~8, which resulted in the time step of 10e-5 s. After a certain number of iterations when the tank level has been stabilized, the simulation was continued with an increased Courant number, which resulted in the time step of 10e-3 s.

2.3 Numerical grid study

A grid independence test was carried out to discover the optimum grid size for the present study. The mesh cross-section of the numerical model and the locations of cross-sections of the velocity profiles are shown in Fig 2.

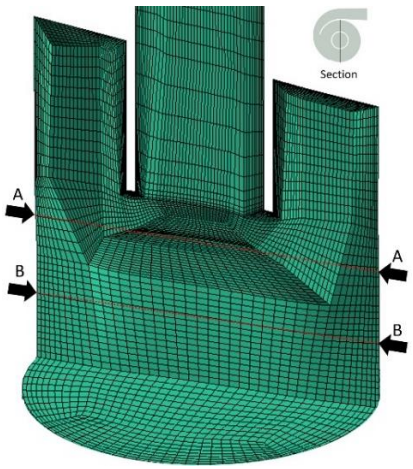

Fig. 2 Mesh at the cross-sections of the separator (center and bottom exit)

The separator geometry was discretized using the Ansys ICEM 19.2 package and the present analysis was performed using a hexa-type mesh. The mesh pattern was prepared as vertical and coincident with the flow direction. The grid independence study considered four meshes with 238k, 613k, 1113k and 1714k elements. The mesh density was increased uniformly in the whole domain of the separator. The quality of all 3D computational meshes was above 0.3. The value of y-plus for all the meshes was about 30. Four parameters were considered for the mesh study: the separator pressure drop, the

oil quality, efficiency and the oil tank filling level. In addition, the axial velocity and the circumferential velocity for cross-section A were compared. The 238k elements mesh showed an about 49% lower oil tank filling level compared to the finest mesh. The mesh with 613k elements showed a 10% difference in pressure drop compared to 1113k elements and higher. It was found that there was no significant change in the separator efficiency and beyond the grid size of 613k, the oil quality was not changed for more than 1%.

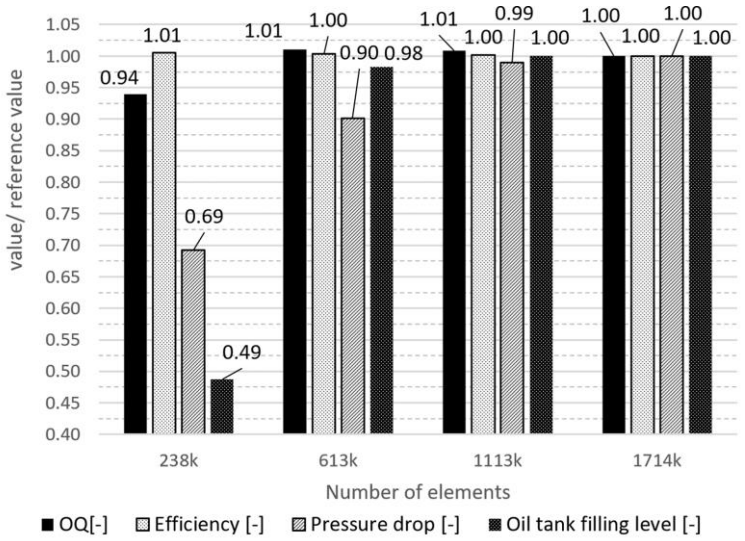

Fig. 3 Mesh impact on the analyzed parameters (reference value for 1714k mesh)

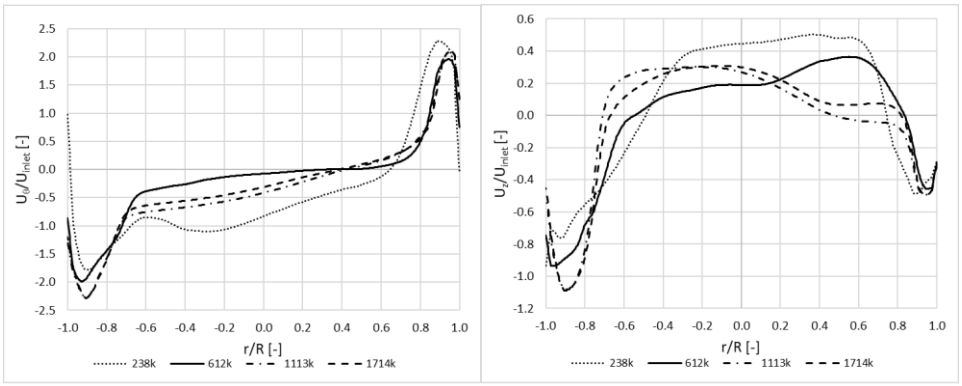

A B

Fig. 4 Velocity profiles: A) Tangential velocity over separator inlet velocity (cross-section A); B) Axial velocity over separator inlet velocity (cross-section A)

Mesh with 1113k elements showed comparable values of all four parameters compared to mesh 1714k (Fig. 3). The velocity results showed that the difference

between the 1113k grid and the finest grid for peak velocities near the wall was below 0.3% (Fig. 4A-B). However, a very fine mesh requires significantly larger computational resources and time while there is no experimental data that can be used for validation. Considering the difference in parameters, the mesh with 613k elements was selected for the numerical study. Since the main objective of this study is to investigate the effects of the gas-liquid free interface on the flow field and performance, the selected mesh guarantees acceptable accuracy of the results in a reasonable computing time.

2.4 Test rig arrangement

The test bench created for the evaluation of the static deaerator efficiency is shown in Fig. 6. The oil used in the test complied with the MIL-L-23699 specification. The air-oil ratio can be set as engine conditions [6]. The oil temperature is limited to the engine normal operating conditions (no overheating). Altitude conditions cannot be simulated. The separator is located in a dummy tank with a system measuring the oil level inside the tank. The tested object is in its original dimensions with the possibility of being reused in the aircraft engine. The oil flow is managed by the rig gear pump (2) with its rotational speed adjustable by a frequency inverter. Airflow is provided by an external system of the test facility. The air mass flow rate and the oil volumetric flow rate are measured.

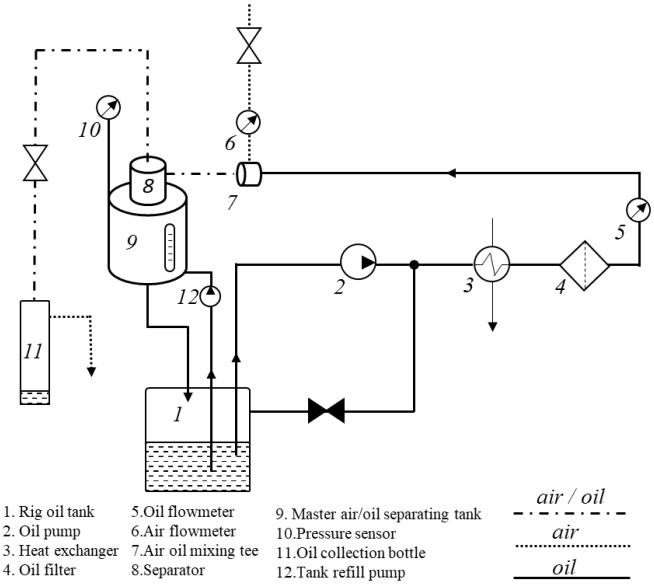

Fig. 5 Diagram of the test bench

In the experiment, the volumetric air/oil ratio at the inlet was equal to 0.4. The oil-air mixture is generated by the mixing tee (7). Separated oil returns to the tank (1), which is several times bigger than the master tank (9) to ensure degassing of the oil delivered for separation. The oil level in the reservoir (11) and the time of the level rising are monitored. Due to that, the oil loss flow rate can be established. The oil tank filling level (OTFL) is defined by:

$$OTFL = \frac{W_{oil}}{W_{total}} \tag{8}$$

where W_{oil} is the mass of oil in the calculation domain and W_{total} is the total mass possible accumulated in the domain.

The performance of the separation process, which is the object of this calculation, is described by two coefficients (cf. Eq. (10-11)). Oil separation efficiency η_s is estimated by Eq. (10) determined by oil trapping in the oil collection bottle ($\dot{V}_{o,vent}$).

$$\eta_s = \frac{\dot{V}_{o,inlet} - \dot{V}_{o,vent}}{\dot{V}_{o,inlet}} \tag{10}$$

The oil quality coefficient (OQ) is defined as the ratio of the oil volumetric flow rate at the separator inlet to the sum of the volumetric flow rate of air at the bottom outlet and the volumetric flow rate of oil at the separator inlet.

$$OQ = \left(\frac{\dot{V}_o}{\dot{V}_a + \dot{V}_o}\right)_{oil\ outlet} \tag{11}$$

The test was performed for the selected engine operating conditions. First, the flow of oil was initiated to obtain the right temperature. Then, the oil level in the tank was determined. The next step involved providing air to the T-pipe. The tank was refilled with to maintain constant level of the separated oil.

3. Results and Discussion

3.1 Determination of the separator performance

During the experimental tests, both the quality of oil and the separator performance were determined depending on the oil level in the tank. While testing, it turned out that a low level of oil (below 50%) caused uncovering the tank oil outlet and drawing in large volumes of air, which led to a significant decrease of the oil quality.

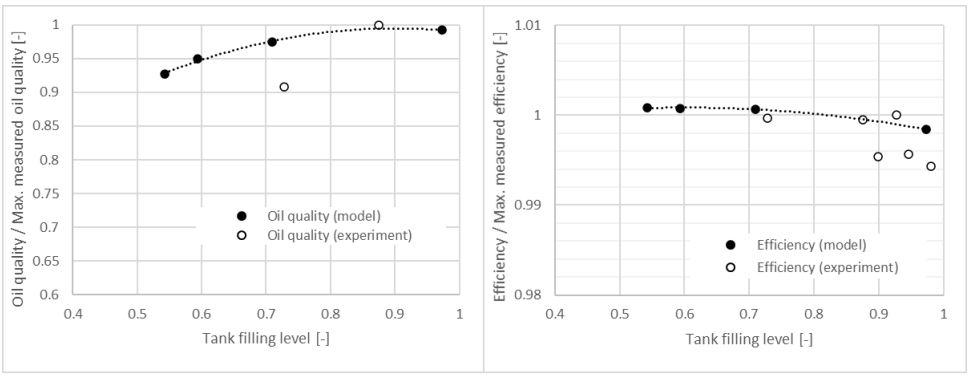

A B

Fig. 6 Separator performance: A) oil quality results vs. tank filling level; B) efficiency vs. tank filling level

Due to the above, the analysis was performed for the oil level range between 50% and 100%. In Fig.6A, it was observed that the greater the tank filling level, the higher the oil quality. The experimental data showed 10% decrease in the oil quality at the mid-point of the studied range. According to the numeric model calculations, the decrease was ~8% for the entire range. The difference between the experimental results and the computed values was only 1%, in the range with higher filling levels. For the lower tank filling level this difference was greater and was about -5% compared to the model values.
The results obtained comply with the model presented in [5], because the greater filling level increases the retention time of oil particles in the tank. During normal operation, air bubbles have more time to separate in the bottom part of the tank. Oil sloshing in the tank also affects the oil quality. At a lower oil level, this phenomenon negatively affects the air separation in the tank because the stream of oil which leaves the separator splashes on the bottom, which may cause undesired repeated aerating.

The subsequent experiment results showed decreased separator performance as the oil level in the tank grew. The separator performance drop reached ~0.57% in the experiment and was higher than the performance drop determined by the numerical model (~0.24%). At the lower oil level, the values obtained were similar to the model assumptions; however, above the level of 0.9 the deviation from the model value was about ~0.4%. There was also growing dispersion of points when the filling level was high. The numerical model provides similar performance values within the filling range of 0.7-0.8 (Fig. 6B).

3.2 Characteristic of free surface and oil fraction

The performed simulations for different filling levels revealed that a free surface and a layered structure of oil fractions were formed in the tank. It was observed that the lowest oil surface was localized in its axis and the highest was by the tank walls – it was caused by the liquid rotary motion (Fig. 7). The author's observations are consistent with the separator tests performed in the petrochemical industry (Fig. 7). The performance drop as a consequence of the increased volume of oil flowing out through the vortex

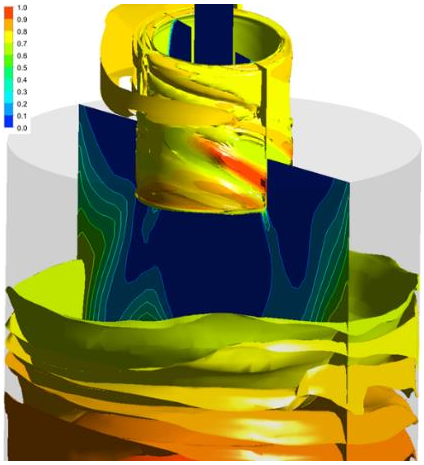

Fig. 7 Oil volume fraction iso surface

finder (Eq. 10) was caused by the approach of the free surface to the vortex finder and the decreased height of the inner vortex.

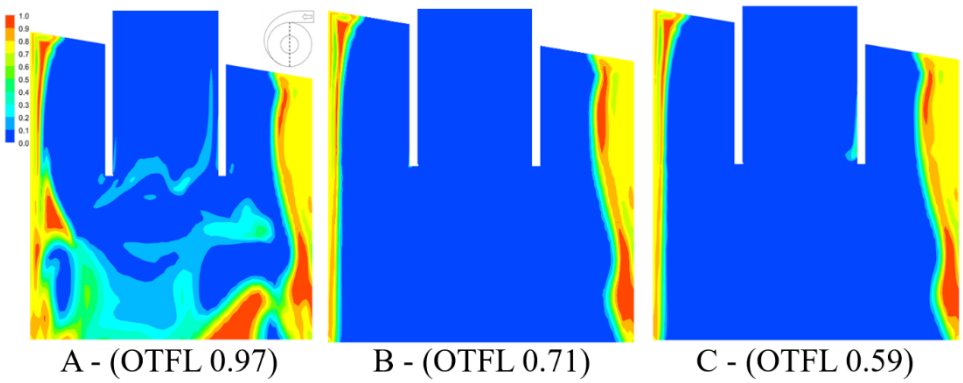

Fig. 8 Oil volume fraction contours for different oil tank filling levels

Further analyses focused on the time-average oil fraction contours for 3 different tank filling levels. The oil film pattern inside the cyclone had an asymmetric profile. The oil phase concentrated in the same regions and layers of oil fractions were created in the same way. It was shown that the high oil level OTFL 0.97 led to a greater number of oil fractions (0.2-0.6) in the internal parts of the separator (Fig. 8A). The increased amount of oil fraction in the separator inner part decreased the performance because part of the oil would be drawn through the outlet. Oil flow through the separator vent was non-stationary. For OTFL 0.71, there was oil fractions outflow (Fig. 8B), but it was visible for OTFL 0.59 (Fig. 8C). The oil which flows back to the separator disturbed the formation of the oil film on the separator walls only for OTFL 0.97 (Fig. 8A), whereas for other levels the oil fraction contours were similar and did not show distortions (Fig. 8B-C). Further observations of the oil fraction contours revealed three concentration sites – the top left-hand corner and the top and bottom right-hand corner. In the top left-hand corners, the concentration of oil results from its accumulation due to tangential velocity and gas flow over the inlet, and it causes oil to rise. This phenomenon is not desired due to mixture recirculation. Another concentration site is in the top right-hand corners where the oil fraction layer is the thickest, but air separation is low. In all cases, the highest oil concentration was also observed in the bottom right-hand corner. It results from the separation of oil due to the rotary motion and formation of the spiral flow down the outlet (Fig. 8A-C).

3.3 Velocity fields and profiles

In the next stage, the observation was focused on the tangential and axial velocity field. It was shown that the flow inside the separator was highly dependent on the tangential inlet geometry and the highest tangential velocity was recorded close to the inlet region. It was confirmed in the tests performed by Erdal et al. [4]. On the left side of the separator, in turn, the velocity field was uniform at its whole height (Fig. 9A-C).

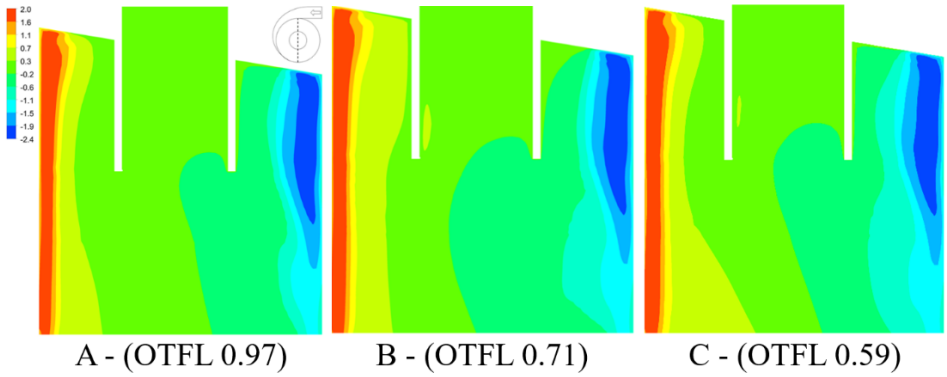

Fig. 9 Tangential velocity contours for different oil tank filling levels

The tangential velocity values in A and B sections were then analyzed. The velocity profile was divided into 4 ranges. The first was close to the wall where the velocity was almost zero due to the wall skin friction. The second was where the forced vortex occurs, in which the velocity grew significantly and reached the maximum. In the third range, the tangential velocity decreased linearly to the value of about 0.5. The fourth range was close to the vortex finder and the velocity dropped to 0.

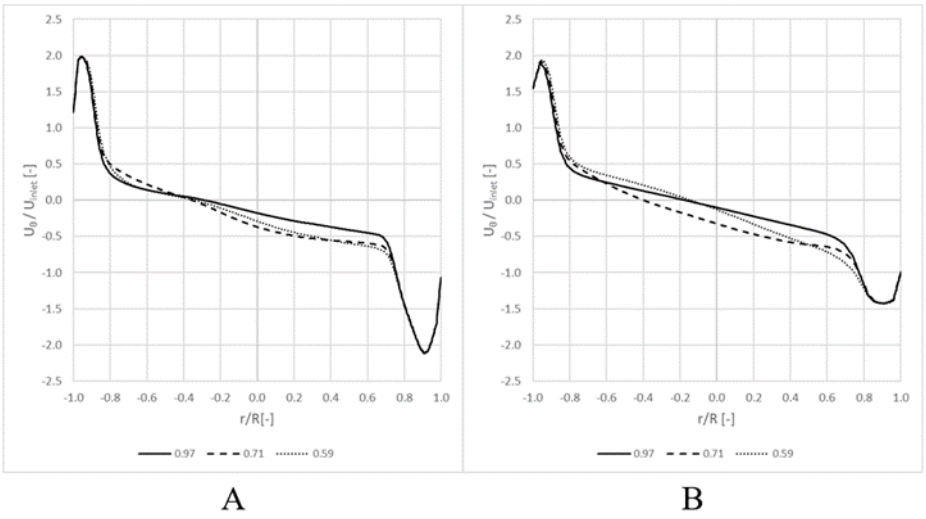

Fig. 10 Tangential velocity at sections A and B

The highest velocity was recorded in the inlet region in the A section, and it decreased near the separator vortex finder (B section). Velocity on the left side of the separator section was similar in all cases.

The oil level in the tank had no significant impact on the velocity in the second range. The difference in velocity in the last two ranges (-0.8÷0.8 r/R) was noticeable but its value was insignificant (about ~0.25). It should be noted that the tangential velocity

profile presented in Fig. 10A-B is nearly symmetrical about the center of the separator is the same as presented in [4].

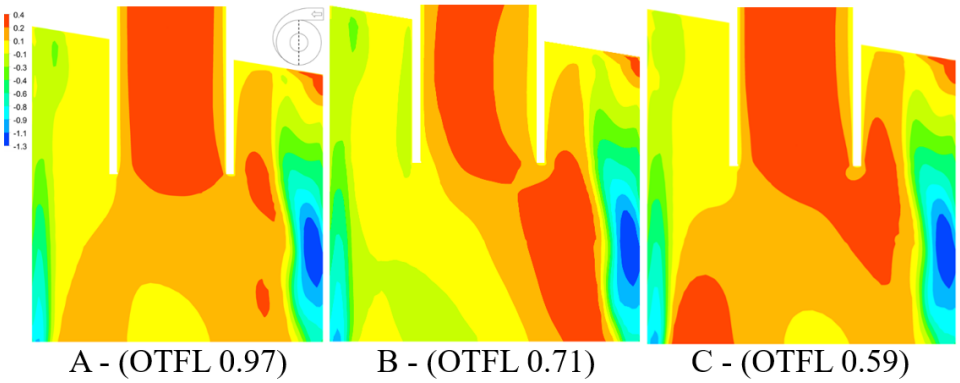

Fig. 11 Axial velocity contours for different oil tank filling levels

Another investigated parameter was the axial speed. Differences between the contours, connected with the unstable flow within the separator were observed. It was noted that the highest velocity was where the oil phase concentrated on the wall in the bottom right-hand corners. The gas flow velocity in the core was three times lower than by the walls. There was also an asymmetrical flow in the vortex finder, caused by the non-axial location of the top outlet against the bottom outlet (Fig. 11).

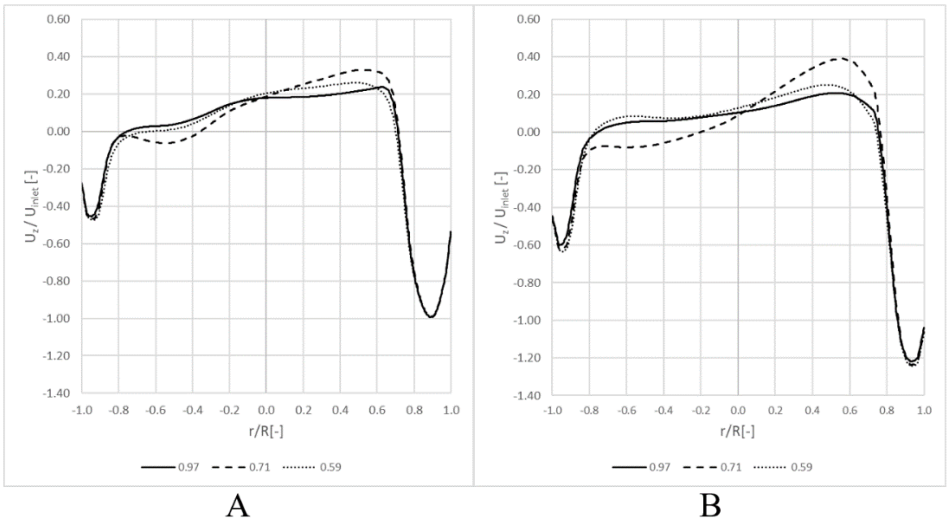

Fig. 12 Axial velocity for sections A and B

Next, axial velocity profiles for sections A and B were evaluated. The velocity of the mixture by the inner walls was turned downward towards the separator outlet, and as it deviated from the wall towards the separator axis, it turned upwards to the vent line.

The values calculated indicated a strong flow along the cyclone walls. It is of key significance for the separation process because this mechanism plays a dominant role in removing the separated oil-air mixture. Within the second range, the flow turned into the opposite direction and, as a result, there was z place where the axial velocity was 0 – the so-called locus zero. In the studied geometry the locus zero is found at values r/R of ~-0.8 and ~0.7 (Fig. 12A-B).

4. CONCLUSION

The publication presents a CFD analysis of the air-oil separator used in a turbine aircraft engine. The simulation was performed for one set of boundary conditions. The VOF model and the RNG k-ε turbulence model used allow simulating the complex interfacial surface shape in the separator. It refers to both the free surface of the oil in the tank and the surface of the oil structures in the separators. The proposed hexagonal grid was effective in modeling the two-phase flows in the oil separator.

The oil quality and the separator performance were calculated numerically for different filling levels and compared with the test results to validate the calculation model. The results obtained show that in the bottom filling range the performance complies with the measurements and there is a difference in the oil quality values, whereas in the top filling range it is the opposite – the oil quality values are similar while separator performance values are different. Based on the results obtained, it was concluded that the increase in the oil level above 0.9 may decrease the separator performance by about 0.5% but it helps obtain the oil quality above 95%.

In the case presented herein, the optimal filling level which would allow maintaining properly high oil quality and performance is 70-90%.

The tangential and axial velocity profiles were examined for the simulated boundary conditions. The tests did not show that the filling level affects the profiles of the average velocity components. Due to the lack of experimental data, the profiles obtained were compared to the ones described in GLCC literature. The behavior of the velocity profile was consistent with the test results for the separators used in the petrochemical industry. For future tests, it would be important to verify the oil quality experimental results while adopting a different measuring approach. As the next step, a check with other engine conditions is planned.

REFERENCES

1. Ippoliti, L., Hendrick, P., 2013, *Influence of the supply circuit on oil pump performance in an aircraft engine lubrication system*, Proceedings of the ASME Turbo Expo 2013: Turbine Technical Conference and Exposition, San Antonio, USA, June 3-7, 2013, doi: 10.1115/GT2013-94500
2. Yanovskiy, L., Ezhov, V., Molokanov, A., 2016, *The foaming properties of lubricating oils for aircraft gas turbine engines*, 30th Congress of the International Council of the Aeronautical Sciences, Daejeon, Korea, September 25-30, 2016.
3. https://patents.google.com/patent/US9033690B2 (last access: 26.01.2022)

4. Erdal, F.M., Shirazi, S.A., Shoham, O., Kouba, G.E., 1997, *CFD simulation of single-phase and two-phase flow in gas-liquid cylindrical cyclone separators*, SPE Journal, 2(4), pp. 436-446.
5. Kristoffersen, T., Holden, C., Skogestad, S., Egeland, O., 2017, *Control-oriented modelling of gas-liquid cylindrical cyclones*, American Control Conference, Seattle, USA, May 24-26, 2017, doi: 10.23919/ACC.2017.7963380
6. Tauber, T., D'Ambrosia, S., Rudbarg, F., 1982, *A lube system diagnostic monitor with deaeration capability*, ASME 1982 International Gas Turbine Conference and Exhibit, London, England, April 18-22, 1982, doi: 10.1115/82-GT-79
7. Ma, L., Qian, P., Wu, J., Bai, Z., Yang, Q., 2013, *Simulation and analysis of 75mm gas-liquid cyclone flow field*, AASRI Winter International Conference on Engineering and Technology, doi: 10.2991/wiet-13.2013.24
8. Qian, P., Ma, L., Liu, Y., Zhang, Y., 2013, *Numerical study of gas-liquid micro-cyclone separator flow field*, AASRI Winter International Conference on Engineering and Technology, doi: 10.2991/wiet-13.2013.27.
9. Zhu, W., Hu, L., Zhang, X., 2019, *The effects of the lower outlet on the flow field of small gas–liquid cylindrical cyclone*, Proceedings of the Institution of Mechanical Engineers, Part C: Journal of Mechanical Engineering Science, 233(4), pp. 1262-1270.
10. Erdal, F.M., Shirazi, S.A., Mantilla, I., Shoham, O., 1998, *CFD study of bubble carry-under in gas-liquid cylindrical cyclone separators*, SPE Annual Technical Conference and Exhibition,New Orleans, September 27-30, 1998, doi: 10.2118/49309-MS.
11. Gomez, L., Mohan, R., Shoham, O., 2004, *Swirling gas–liquid two-phase flow — experiment and modelling part I: swirling flow field*, Journal of Fluids Engineering, 126(6), pp. 935-942.
12. Arpandi, I., Joshi, A.R., Shoham, O., Shirazi, S., Kouba, G.E., 1996, *Hydrodynamics of two-phase flow in gas-liquid cylindrical cyclone separators*, SPE Journal, 1(4), pp. 427-436.
13. Mantilla, I., Shirazi, S.A, Shoham, O., 1999, *Flow field prediction and bubble trajectory model in gas-liquid cylindrical cyclone (GLCC) separators*, Journal of Energy Resources Technology, 121(1), pp. 9-14.
14. Gomez, L., Mohan, R.S., Shoham, O., Kouba, G.E., 2000, *Enhanced mechanistic model and field-application design of gas/liquid cylindrical cyclone separators*, SPE Journal, 5(2), pp. 190-198.
15. Chirinos, W.A., Gomez, L., Wang, S., Mohan, R.S., Shoham, O., Kouba, G.E., 2000, *Liquid carry-over in gas/liquid cylindrical cyclone compact separators*, SPE Journal, 5(3), pp. 259-267.
16. Erdal, F.M., Shirazi, S.A., 2004, *Local velocity measurements and computational fluid dynamics (CFD) simulations of swirling flow in a cylindrical cyclone separator*, Journal of Energy Resources Technology, 126(4), pp. 326-333.
17. Kouba, G.E., Wang, S., Gomez, L., Mohan, R., Shoham, O., *Review of the state-of-the-art gas/liquid cylindrical cyclone (GLCC) technology-field applications*, International Oil & Gas Conference and Exhibition, Beijing, China, December 5-7, 2006, doi: 10.2523/104256-MS.
18. Kefalas P., Margaris D.P., 2007, *CFD study of a novel compact phase separator*, 2nd International Conference on Experiments/Process/System Modelling/Simulation & Optimization, Athens, Greece, July 4-7, 2007.
19. Hirt, C.W., Nichols, B.D., 1981, *Volume of fluid (VOF) method for the dynamics of free boundaries*, Journal of Computational Physics, 39(1), pp. 201-225.
20. Szwarc, T., Wróblewski, W., Borzęcki, T., 2020, *Analysis of a cylindrical cyclone separator used in aircraft turbine engine*, Technical Science, 23(2), pp. 131-142.
21. Yakhot, V., Orszag, S.A., 1986, *Renormalization group analysis of turbulence. I. Basic theory*, Journal of Scientific Computing, 1(1), pp. 3-51.
22. Wang, L.Z., Gao, X., Feng, J.M., Peng, X.Y., 2015, *Research on the two-phase flow and separation mechanism in the oil-gas cyclone separator*, IOP Conference Series: Materials Science and Engineering, 90, 012075.